

# Impact of cation size on magnetic properties of $(AA')_2\text{FeReO}_6$ double perovskites

J. M. De Teresa, D. Serrate, J. Blasco, M. R. Ibarra, and L. Morellon

*Instituto de Ciencia de Materiales de Aragón, Universidad de Zaragoza-CSIC, Facultad de Ciencias, 50009 Zaragoza, Spain*

(Received 6 June 2003; revised manuscript received 5 December 2003; published 1 April 2004)

We study the influence of the cation size in the magnetic properties of  $(AA')_2\text{FeReO}_6$  ( $AA' = \text{Ba}_2, \text{Ba}_{1.5}\text{Sr}_{0.5}, \text{BaSr}, \text{Ba}_{0.5}\text{Sr}_{1.5}, \text{Sr}_2, \text{Ca}_{0.5}\text{Sr}_{1.5}, \text{CaSr}, \text{Ca}_{1.5}\text{Sr}_{0.5}, \text{Ca}_2$ ) double perovskites. As the average cation size decreases, the crystallographic structure at room temperature evolves from cubic to tetragonal and monoclinic. The large lattice effects observed for the monoclinic compounds could be responsible for their anomalous behavior. The Curie temperature increases anomalously from  $\approx 303$  K for  $\text{Ba}_2$  to  $\approx 522$  K for  $\text{Ca}_2$ , which seems to need an additional ferromagnetic coupling to the usual  $(\text{Fe } t_{2g} - \text{Re } t_{2g})$   $pdd-\pi$  coupling. At 5 K, the magnetization at 5 T is close to  $3\mu_B/\text{f.u.}$  for those compounds with average cation size between that of  $\text{Ba}_2$  and that of  $\text{Ca}_{0.5}\text{Sr}_{1.5}$  and the coercivity is found to be large in all cases (in the KOe range). The remaining compounds ( $\text{CaSr}, \text{Ca}_{1.5}\text{Sr}_{0.5}, \text{Ca}_2$ ) undergo a simultaneous structural and magnetic transition below 150 K which produces a huge increase in the coercivity and reduces the magnetization. Magnetotransport properties change accordingly. From our results, a novel strong magnetostructural coupling in these compounds is anticipated. These results are interpreted within a scenario where the Re orbital state plays a crucial role in the ground state.

DOI: 10.1103/PhysRevB.69.144401

PACS number(s): 75.30.Kz, 75.30.Cr, 72.25.Mk, 61.12.Ld

## I. INTRODUCTION

Magnetic oxides with an ordered double-perovskite structure  $A_2BB'O_6$  are very promising for applications in the field of spin electronics. In order to build real devices working at and above room temperature, stringent requirements are a high spin polarization at the Fermi level together with a high Curie temperature ( $T_C$ ), far above room temperature. After the discovery of those properties in  $\text{Sr}_2\text{FeMoO}_6$  ( $T_C = 410$  K),<sup>1</sup> other ordered double perovskites  $A_2BB'O_6$  ( $A = \text{Ca}, \text{Sr}, \text{Ba}, \text{La}, \text{etc.}; BB' = \text{FeMo}, \text{FeRe}, \text{CrRe}, \text{CrW}, \text{etc.}$ ) are being intensively studied at the aim of finding a compound with even better performance.<sup>2–13</sup> Some devices based on  $\text{Sr}_2\text{FeMoO}_6$  like magnetic tunnel junctions<sup>14</sup> and magnetoresistive potentiometers<sup>15</sup> have already been produced.

The ferromagnetic metallic properties of  $\text{Sr}_2\text{FeMoO}_6$  have been explained by the double-exchange interaction Fe-O-Mo. Band calculations indicate that, with regard to the valence and conduction bands, the spin-up subband is below the Fermi level and consists of five “localized” 3d electrons produced by Fe ( $S = 5/2$ ). The spin-down subband would be located at the Fermi level and would consist of one “delocalized” electron shared by Fe and Mo and mediating the double-exchange interaction between the “localized” spins through the oxygen orbitals.<sup>1</sup> Ideally, the conduction electrons would show complete negative spin polarization at the Fermi level, say, half metallicity. This property would lie at the basis of the high tunnel magnetoresistance observed in magnetic tunnel junctions due to spin-polarized tunneling<sup>14</sup> and in polycrystalline samples due to the intergrain magnetotunnelling effect.<sup>1</sup>

Re-based double perovskites are the most promising compounds in terms of high  $T_C$ .<sup>7–13</sup> Thus, the compound  $\text{Sr}_2\text{CrReO}_6$  is found to have  $T_C \approx 635$  K and the compound  $\text{Ca}_2\text{FeReO}_6$  is found to have  $T_C \approx 538$  K. However, these compounds show structural, magnetic and transport properties substantially different from those of the archetypal

$\text{Sr}_2\text{FeMoO}_6$  compound. Thus, when comparing  $\text{Ca}_2\text{FeReO}_6$  and  $\text{Sr}_2\text{FeMoO}_6$ , we notice that with regard to structural properties,  $\text{Ca}_2\text{FeReO}_6$  is monoclinic, and  $\text{Sr}_2\text{FeMoO}_6$  is tetragonal. Wu proposed that the lower Fe-O-Re angle in  $\text{Ca}_2\text{FeReO}_6$  ( $\sim 156^\circ$  at room temperature<sup>7</sup>) than in  $\text{Sr}_2\text{FeMoO}_6$  ( $\sim 172^\circ$  at room temperature<sup>16</sup>) could be at the origin of the increased  $T_C$  in  $\text{Ca}_2\text{FeReO}_6$  by allowing a  $pdd-\sigma$  coupling.<sup>17</sup> When comparing the electronic structure of both compounds, we also notice that the Re brings about more electrons to the spin-down subband,<sup>17</sup> which can also be a source for increasing  $T_C$ .<sup>5,18</sup> Especially intriguing is the difference in the magnetic behavior. Re-based double perovskites are magnetically hard,<sup>11,19</sup> which is not the case in Mo-based double perovskites.<sup>1</sup> Regarding the transport properties,  $\text{Ca}_2\text{FeReO}_6$  shows semiconducting behavior<sup>8</sup> in contrast with the metallic behavior of  $\text{Sr}_2\text{FeMoO}_6$ .<sup>1</sup> In addition,  $\text{Ca}_2\text{FeReO}_6$  undergoes a structural transition below  $T_S \sim 150$  K that further increases its resistivity.<sup>12,13,20</sup> All these properties make the study of  $\text{Ca}_2\text{FeReO}_6$  very appealing. However, it seems clear that systematic studies are necessary in order to understand the unexpected properties of Re-based double perovskites.

In our study, we have systematically varied the cation size in  $(AA')_2\text{FeReO}_6$  double perovskites by synthesizing the compounds  $AA' = \text{Ba}_2, \text{Ba}_{1.5}\text{Sr}_{0.5}, \text{BaSr}, \text{Ba}_{0.5}\text{Sr}_{1.5}, \text{Sr}_2, \text{Ca}_{0.5}\text{Sr}_{1.5}, \text{CaSr}, \text{Ca}_{1.5}\text{Sr}_{0.5}, \text{Ca}_2$ . The wide range of cation sizes used has allowed us to investigate how the structural, magnetic, and magnetotransport properties change from  $\text{Ba}_2\text{FeReO}_6$ , a cubic system showing metallic behavior, low Curie temperature, and not too large coercivity, to  $\text{Ca}_2\text{FeReO}_6$ , a monoclinic system showing semiconducting behavior, high Curie temperature, and huge coercivity. Our work focuses on the influence of the cation size on the magnetic properties, which will simultaneously impact on lattice effects and magnetotransport properties. In fact, our results anticipate a novel magnetostructural coupling in these com-

pounds which is explained by the relevant role played by an unquenched Re orbital magnetic moment in combination with the spin-orbit coupling and crystal-field effects.

## II. EXPERIMENTAL DETAILS

The samples were prepared by solid state reaction. Stoichiometric amounts of  $A_2CO_3$  ( $A = \text{Ba}, \text{Sr}, \text{and Ca}$ ),  $\text{Fe}_2\text{O}_3$ ,  $\text{ReO}_3$ , and Re (the  $\text{ReO}_3/\text{Re}$  ratio is 5/1), were mixed and pressed into pellets. The pellets were heated at  $1000^\circ\text{C}$  during 3 h in an atmosphere of Ar (nominal purity 99.9995%) with heating and cooling rates of  $7^\circ\text{C}/\text{min}$ . Contact between pellets and crucible are minimized to avoid Re loss. The resulting pellets were soft and usually showed breaks but the perovskite phase was already formed. As the electrical measurements require hard samples without breaks, a part of each sample was ground, pelletized and sintered at  $1000^\circ\text{C}$  during 1 h. The new pellets were harder and did not show changes in their physical properties.

X-ray measurements have been performed with a D-max Rigaku system with rotating anode operated at 40 kV and 80 mA and a graphite monochromator was used to select the  $\text{Cu } K\alpha_{1,2}$  radiation. For the low-temperature x-ray measurements, a cryostat working down to liquid nitrogen temperature has been used. Structural data have been obtained from refinement of the x-ray diffraction patterns by using FULLPROF. The Curie temperature has been measured by means of a Faraday balance working above room temperature. Magnetization measurements up to 50 KOe across the temperature range 5–375 K have been carried out in a commercial superconducting quantum interference device magnetometer. Magnetotransport properties have been measured by the four-point technique by injecting a dc current and measuring the voltage across the central contacts, either keeping current or voltage constant for low and high resistances, respectively. Thermoelectric effects are minimized by inverting the current. Magnetic field up to 1.5 T for the magnetoresistance measurements was provided by an electromagnet.

## III. RESULTS

Refinements of the x-ray diffraction patterns at room temperature indicate that the samples are single phase except for the presence of tiny amounts of impurity phases. A usual impurity, hardly detected in the x-ray patterns (and not always), is metallic Re in amounts equal or less than 0.6%. Only  $\text{Ba}_2\text{FeReO}_6$  showed asymmetric broadening in the base of the main diffraction peaks that may be related to the presence of a minor secondary perovskite phase poorly crystallized. Concerning the crystal and magnetic structure of  $\text{Ca}_2\text{FeReO}_6$ , Westerburg *et al.* claim phase separation in two different phases across a wide temperature range<sup>12</sup> while Oikawa *et al.* find single phase behavior at room temperature.<sup>21</sup> This difference could be related to details of the synthesis. Our synthetic route is similar to that one reported by Oikawa *et al.*<sup>21</sup> and is characterized by a short reaction time and the use of Re plus Re oxides ( $\text{ReO}_3$ ) instead of Fe plus  $\text{Fe}_2\text{O}_3$  as precursors in order to achieve a mixed valence state. In our  $\text{Ca}_2\text{FeReO}_6$  sample we have not

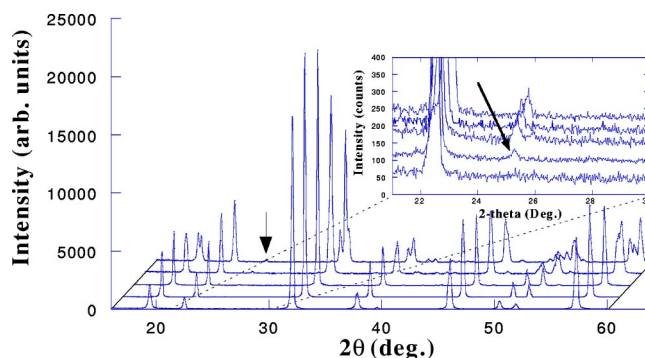


FIG. 1. X-ray diffraction patterns at room temperature of the  $AA' = \text{Sr}_2$ ,  $\text{Ca}_{0.5}\text{Sr}_{1.5}$ ,  $\text{CaSr}$ ,  $\text{Ca}_{1.5}\text{Sr}_{0.5}$ , and  $\text{Ca}_2$  compounds (shown in this order in the figure). The inset shows in detail the  $2\theta$  range where the (111) peak appears and marks the appearance of the  $P2_1/n$  monoclinic structure (see text).

found any evidence for phase separation at room temperature. The corresponding pattern was successfully refined with one crystallographic phase and giving rise to structural parameters similar to those ones reported by Oikawa *et al.*<sup>21</sup>

The compounds  $AA' = \text{Ba}_2$ ,  $\text{Ba}_{1.5}\text{Sr}_{0.5}$ ,  $\text{BaSr}$ , and  $\text{Ba}_{0.5}\text{Sr}_{1.5}$  show cubic structure (space group  $Fm\bar{3}m$ ) whereas  $\text{Sr}_2$  is tetragonal (space group  $I4/m$ ) and  $\text{Ca}_{0.5}\text{Sr}_{1.5}$ ,  $\text{CaSr}$ ,  $\text{Ca}_{1.5}\text{Sr}_{0.5}$ , and  $\text{Ca}_2$  are monoclinic (space group  $P2_1/n$ ). These structural phase transitions can be understood by taking into account that a smaller cation size favors the tilting of the Fe/Re-O octahedra in order to fill the empty space around the cations and the cubic structure is replaced by other space groups with lower symmetry. For example, the  $I4/m$  space group arises from the  $a^0a^0c^-$  octahedral tilt (Glazer's terminology<sup>22</sup>) whereas the  $P2_1/n$  space group arises from the  $a^+b^-b^-$  tilt. The tilts give rise to small displacements of the oxygen atoms from the ideal cubic positions and new diffraction peaks come up. Figure 1 shows the room-temperature x-ray diffraction patterns for  $AA' = \text{Sr}_2$ ,  $\text{Ca}_{0.5}\text{Sr}_{1.5}$ ,  $\text{CaSr}$ ,  $\text{Ca}_{1.5}\text{Sr}_{0.5}$ , and  $\text{Ca}_2$ . The monoclinic distortion of the unit cell is clearly visible for  $\text{Ca}_2$  and  $\text{Ca}_{1.5}\text{Sr}_{0.5}$  samples and the patterns can be well fitted within the framework of the  $P2_1/n$  space group. The patterns of the  $\text{Ca}_{0.5}\text{Sr}_{1.5}$  and  $\text{CaSr}$  compounds resemble the pseudocubic structure. However, a detailed inspection of the patterns evidences the presence of the (111) diffraction peak (see inset of Fig. 1), which is forbidden in the tetragonal  $I$ -type lattice. It can be indexed in a primitive cell, so according to the rest of the series, we have refined the patterns in the  $P2_1/n$  space group. It is worth pointing out that such fittings give better reliability factors than those performed within the  $I4/m$  space group.

We would like to remark that even if the octahedra can undergo relatively large tiltings, the pseudocubic unit cell is only slightly deformed even for the smallest cations. This is illustrated in Fig. 2, where the lattice parameters obtained from the refinements are shown as a function of the cation size [ionic radius taken from tables by Shannon for coordination number equal to 12 (Ref. 23)]. In order to compare the overall behavior across the studied series, for the tetragonal and monoclinic compounds the lattice parameters in the

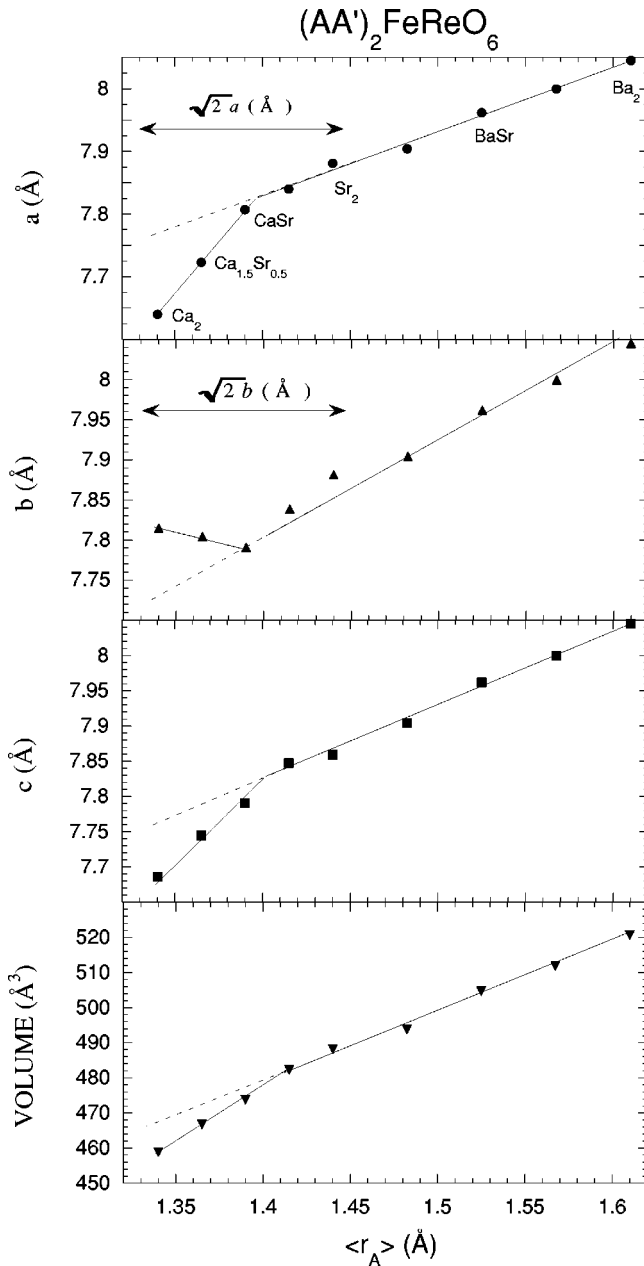


FIG. 2. (a) Cell parameters obtained from x-ray diffraction refinements as a function of the cationic size in  $(AA')_2\text{FeReO}_6$ . In order to establish the overall behavior, in the case of the tetragonal and monoclinic samples ( $AA' = \text{Sr}_2$ ,  $\text{Ca}_{0.5}\text{Sr}_{1.5}$ ,  $\text{CaSr}$ ,  $\text{Ca}_{1.5}\text{Sr}_{0.5}$ ,  $\text{Ca}_2$ ) the lattice parameters  $a$  and  $b$  have been multiplied by  $\sqrt{2}$  (see text). Lines are visual guides. Deviations from a linear behavior occur for the compounds with small cation size.

pseudocubic cell ( $a\sqrt{2}, b\sqrt{2}, c$ ) are represented instead of the parameters of the true unit cell. This is reasonable given the small distortions with respect to the cubic cell. In the case of the monoclinic compounds, the  $\beta$  angle deviates less than  $0.05^\circ$  with respect to  $90^\circ$ . Beginning from  $AA' = \text{Ba}_2$ , the lattice parameters diminish as smaller average cation size is used. A linear dependence is observed from  $AA' = \text{Ba}_2$  to  $AA' = \text{Ca}_{0.5}\text{Sr}_{1.5}$ . However, large deviations from this linear behavior are noticed for the  $AA' = \text{CaSr}$ ,  $\text{Ca}_{1.5}\text{Sr}_{0.5}$ , and  $\text{Ca}_2$

compounds. The largest effect occurs for  $\text{Ca}_2$ , where the deviation in the lattice parameters and the volume is of the order of  $\sim 1\%$ , which is a huge value in terms of lattice effects. The origin of this effect is mainly steric as a similar structural behavior can be deduced from the values of the lattice parameters in  $(AA')_2\text{FeMoO}_6$ .<sup>16</sup> This huge structural effect can trigger new phenomena such as a different electronic structure or a large magnetoelastic coupling. Substantial changes in the electronic structure at room temperature can be ruled out. For instance, in terms of dc resistivity values, we do not observe relevant difference among compounds such as  $AA' = \text{Ba}_2$ ,  $\text{Sr}_2$ , and  $\text{Ca}_2$ . Optical conductivity measurements by Kato *et al.*<sup>13</sup> in  $AA' = \text{Sr}_2$  and  $\text{Ca}_2$  also find metallic behavior at room temperature with a Drude component. However, several features suggest that this huge lattice effect could switch on a large magnetoelastic coupling. One of these features is seen when comparing the individual behavior of the lattice parameters and the direction of the spontaneous magnetization at room temperature in  $\text{Ca}_2\text{FeReO}_6$  (studied by means of neutron diffraction<sup>20</sup>). Granado *et al.* have found that the spontaneous magnetization axis at room temperature lies in the  $ac$  plane,  $55^\circ$  off the  $a$  axis.<sup>20</sup> By inspection of Fig. 2, we notice that at room temperature the  $a$  and  $c$  axis are contracted whereas the  $b$  axis is expanded. Thus, it seems that the easy magnetization axis could be determined by magnetoelastic effects through the Villari effect (inverse magnetostriction effect) in which strain influences the magnetic state. The most common mechanism explaining magnetostriction effects requires an orbital anisotropic electron charge density (which couples to the lattice via crystal-field effects) and a spin-orbit interaction that couples the orbital and spin magnetic moments.<sup>24</sup> A conclusive argument for a strong magnetoelastic effect in  $\text{Ca}_2\text{FeReO}_6$  (and very probably in  $\text{Ca}_{1.5}\text{Sr}_{0.5}\text{FeReO}_6$  and  $\text{CaSrFeReO}_6$  as well) is the fact that an anomalous thermal expansion of the  $b$  axis starts exactly at  $T_C$ , when a spontaneous magnetization sets in.<sup>20</sup> This assumption will be further supported by the correlation observed at  $T_S$  between the new easy magnetization axis measured with neutron diffraction and the change in the individual lattice parameters (see below). Moreover, the magnetic properties reported below can only be explained assuming a strong magnetoelastic coupling.

The  $T_C$  values as a function of the average ionic radius are shown in Fig. 3. For the compounds with ionic radius size between those of  $AA' = \text{Ba}_2$  and  $\text{Sr}_2$ , a roughly linear increase in  $T_C$  with decreasing ionic radius is observed. This increase can be accounted for by the modification of the bare electronic bandwidth ( $W$ ), which is determined by structural parameters, as was already proposed in the  $(AA')_2\text{FeMoO}_6$  series.<sup>16</sup> In that study the phenomenological relationship  $T_C \propto W \approx \cos \omega / (d_{\text{Fe/Mo-O}})^{3.5}$  was found, where  $\omega$  is the “tilt” angle in the plane of the bond, given by  $\omega = (\pi - \langle \text{Fe-O-Mo} \rangle)$ , and  $d_{\text{Fe/Mo-O}}$  is the Fe/Mo-O bond length. In the case of  $(AA')_2\text{FeReO}_6$ , for the compounds between  $\text{Ba}_2\text{FeReO}_6$  and  $\text{Sr}_2\text{FeReO}_6$ ,  $\cos \omega \approx 1$ , and the decrease in the cation size brings about the decrease of  $d_{\text{Fe/Re-O}}$  which will increase the bare electronic bandwidth and, as a conse-

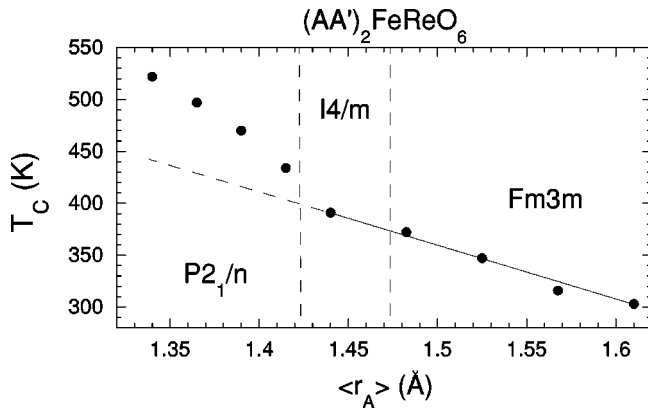


FIG. 3. Crystallographic structure at room temperature and Curie temperature as a function of the average ionic radius at the A site in  $(AA')_2\text{FeReO}_6$ . A linear behavior occurring for large cation sizes breaks for the compounds with cation size smaller than that of  $AA' = \text{Sr}_2$ . Lines are visual guides.

quence,  $T_C$ . However, Fig. 3 clearly shows that with a further decrease in the cation size an additional mechanism must be invoked in order to explain the anomalous increase of  $T_C$  for the compounds between  $\text{Sr}_2\text{FeReO}_6$  and  $\text{Ca}_2\text{FeReO}_6$ . Theoretically, Wu has proposed that deviations of the Fe-O-Re angle from  $180^\circ$  bring about a finite density of states of Fe/Re  $e_g$  orbitals at the Fermi level. This will allow a nonzero (Fe  $e_g$  - Re  $e_g$ )  $pdd$ - $\sigma$  coupling promoting a ferromagnetic interaction. This interaction plus the usual ferromagnetic double exchange interaction via a (Fe  $t_{2g}$  - Re  $t_{2g}$ )  $pdd$ - $\pi$  coupling could enhance the overall ferromagnetic coupling.<sup>17</sup> This assumption can explain Fig. 3 reasonably well, at least qualitatively.

Magnetization measurements (shown in Figs. 4, 5, and 6) have allowed us to investigate the change in some magnetic properties as a function of the cation size. In the simplest ionic picture, two couples of ionic configurations are possible,  $\text{Fe}^{+3}\text{-Re}^{+5}$  and  $\text{Fe}^{+2}\text{-Re}^{+6}$ . Both give an expected saturation magnetization of  $3\mu_B/\text{f.u.}$  Theoretical calculations by Wu<sup>17</sup> predict strong band hybridization but the calculated total spin is  $3\mu_B/\text{f.u.}$  Mössbauer experiments for  $AA' = \text{Ba}_2$  conclude either a  $\text{Fe}^{+3}$  state<sup>25</sup> or a  $\text{Fe}^{+2}$  state<sup>26</sup> or an intermediate valence state between  $\text{Fe}^{+2}$  and  $\text{Fe}^{+3}$  (Ref. 7) and for  $AA' = \text{Sr}_2$  and  $\text{Ca}_2$  a  $\text{Fe}^{+2.5}$  state is proposed.<sup>27</sup> NMR measurements in our samples ( $AA' = \text{Ba}_2$ ,  $\text{Sr}_2$ , and  $\text{Ca}_2$ ) indicate that the Re ions bear a magnetic moment of  $\sim 1\mu_B$ ,<sup>28</sup> which is the expected value for  $\text{Re}^{+6}$ . These NMR measurements also confirm that the Re magnetic moment is antiparallel to the Fe magnetic moment which supports the ferrimagnetic ordering scheme. As a consequence, the expected maximum value for the magnetization in these compounds is  $3\mu_B/\text{f.u.}$

In Fig. 5 the magnetization under 5 T at 5 K is shown as a function of the average ionic radius. At 5 K there are two types of compounds. For large cation sizes ( $AA' = \text{Ba}_2, \text{Ba}_{1.5}\text{Sr}_{0.5}, \text{BaSr}, \text{Ba}_{0.5}\text{Sr}_{1.5}, \text{Sr}_2, \text{Ca}_{0.5}\text{Sr}_{1.5}$ ) its value is close to  $3\mu_B/\text{f.u.}$  in all the compounds as expected from the previous discussion. Deviations from this value in these compounds are normally explained as due to the presence of

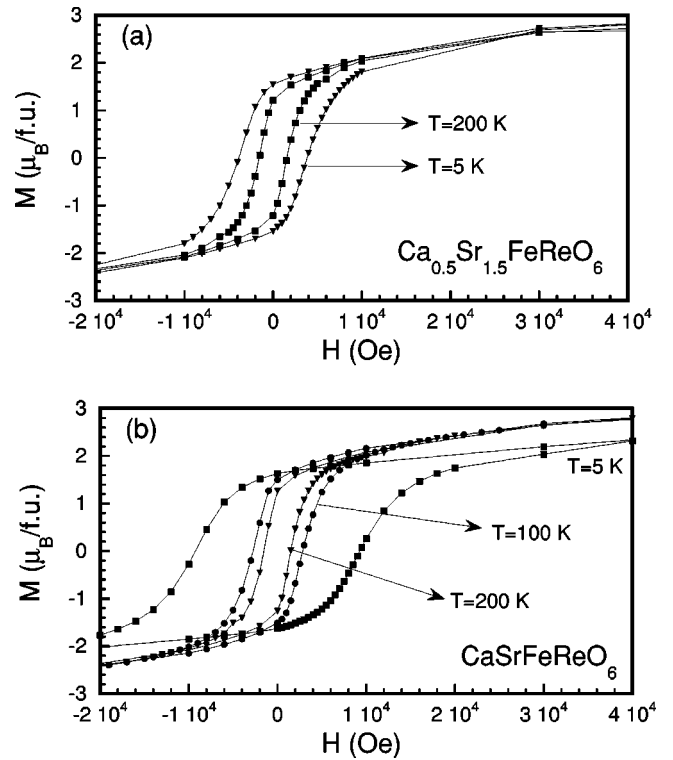


FIG. 4. Magnetization hysteresis loops at selected temperatures for  $\text{Ca}_{0.5}\text{Sr}_{1.5}\text{FeReO}_6$  (a) and  $\text{CaSrFeReO}_6$  (b). The simultaneous structural and magnetic transition in  $\text{CaSrFeReO}_6$  at  $T_S \approx 40$  K produces a decrease in the magnetization under 5 T and a substantial increase in coercivity.

antisite defects.<sup>1</sup> However, for the compounds with small cation size ( $AA' = \text{CaSr}, \text{Ca}_{1.5}\text{Sr}_{0.5}$ , and  $\text{Ca}_2$ ), the magnetization under 5 T is substantially lower than  $3\mu_B/\text{f.u.}$  at 5 K, which correlates with the decrease of magnetization at the simultaneous magnetic/structural transition occurring at  $T_S$ . This transition observed at low temperatures ( $T_S$  below 150 K) in the monoclinic compounds can be detected by means of x-ray diffraction (see Fig. 7) and by measuring the thermal dependence of the magnetization (see Fig. 6). We have defined the exact value of  $T_S$  as the maximum of the derivative of magnetization versus temperature [see Fig. 6(b)]. In Fig. 4 we compare the magnetization loops at temperatures above and below  $T_S$  in two selected compounds. That figure compares  $\text{CaSrFeReO}_6$ ,  $T_S \approx 40$  K, with  $\text{Ca}_{0.5}\text{Sr}_{1.5}\text{FeReO}_6$ , which does not show any transition.  $\text{Ca}_{0.5}\text{Sr}_{1.5}\text{FeReO}_6$  shows a normal behavior in a ferromagnetic material, with slightly larger magnetization and coercivity at 5 K than at 200 K. However, the behavior of  $\text{CaSrFeReO}_6$  is different. First, the magnetization under 5 T decreases below 100 K. Secondly, the coercive field is substantially higher, more than a factor of 3 larger at 5 K than at 100 K, which is not expected from thermal effects alone in a ferromagnetic material. In the case of the  $\text{Ca}_{1.5}\text{Sr}_{0.5}\text{FeReO}_6$  compound, with  $T_S \approx 90$  K, the coercive field increases one order of magnitude from 200 down to 5 K and in the case of  $\text{Ca}_2\text{FeReO}_6$  more than a factor of 4 ( $T_S \approx 110$  K). In order to illustrate this anomalous behavior of the compounds with small cation size, the coercive field is shown in Fig. 5 as a function of the cation size at 200 and 5

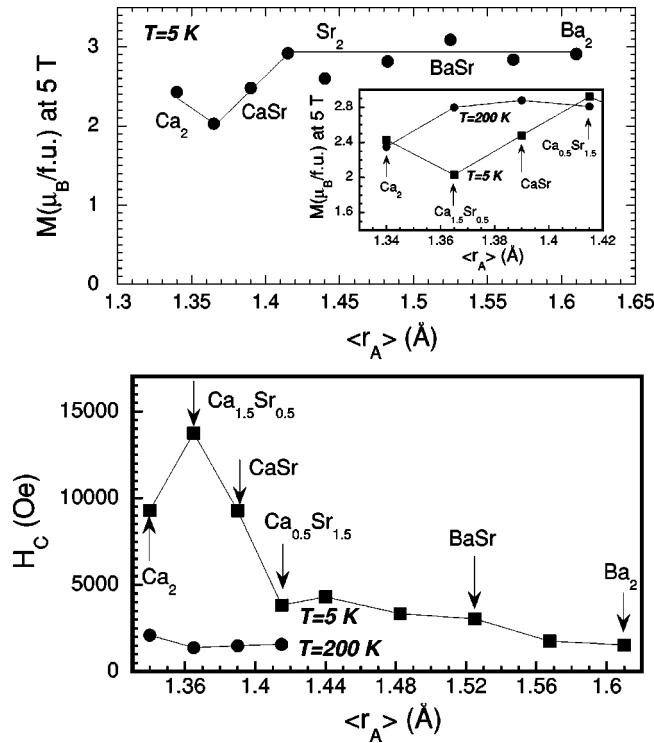


FIG. 5. (a) Magnetization under 5 T and 5 K as a function of the cation size (lines are visual guides). The decrease of magnetization for small cation sizes is connected to a simultaneous structural and magnetic transition occurring below  $\sim 150$  K. The inset compares the magnetization under 5 T at  $T=5$  K and  $T=200$  K for the compounds with small cation sizes. (b) Coercive field as a function of the cation size at  $T=5$  K and  $T=200$  K. The increase of coercivity associated to the magnetic/structural transition is remarkable.

K for all the compounds. These results support the hypothesis of a simultaneous structural/magnetic transition occurring at  $T_S$ . Granado *et al.* have suggested by neutron experiments in  $\text{Ca}_2\text{FeReO}_6$  that below  $T_S$  the easy magnetization axis changes from lying in the  $ac$  plane to be parallel to the  $b$  axis. Moreover, a small diffraction peak, which could correspond to an antiferromagnetic canting in the Re and/or Fe magnetic sublattices with the propagation vector along one particular Fe-Re-Fe binding direction, has been detected.<sup>20</sup> Our results are in agreement with this hypothesis. An antiferromagnetic canting could explain the decrease in the magnetization under 5 T that we observe in  $\text{CaSrFeReO}_6$  and  $\text{Ca}_{1.5}\text{Sr}_{0.5}\text{FeReO}_6$ . In the case of  $\text{Ca}_2\text{FeReO}_6$ , we observe the huge increase in the coercive field at  $T_S$  but we do not observe the decrease in the magnetization under 5 T. A possible reason is that in this sample the transition could be incomplete below  $T_S$ . In fact, neutron diffraction studies evidence a tendency in  $\text{Ca}_2\text{FeReO}_6$  to show mesoscopic phase separation below  $T_S$  in two monoclinic phases, one of them is the high-temperature phase ( $M1$  phase if we adopt the terminology introduced in Ref. 20) and the other one is the low-temperature phase ( $M2$  phase).<sup>12,20</sup> As a consequence, at 5 K the decrease of the magnetization in the  $M2$  phase of  $\text{Ca}_2\text{FeReO}_6$  below  $T_S$  would be compensated by the expected increase of magnetization due to thermal effects in the

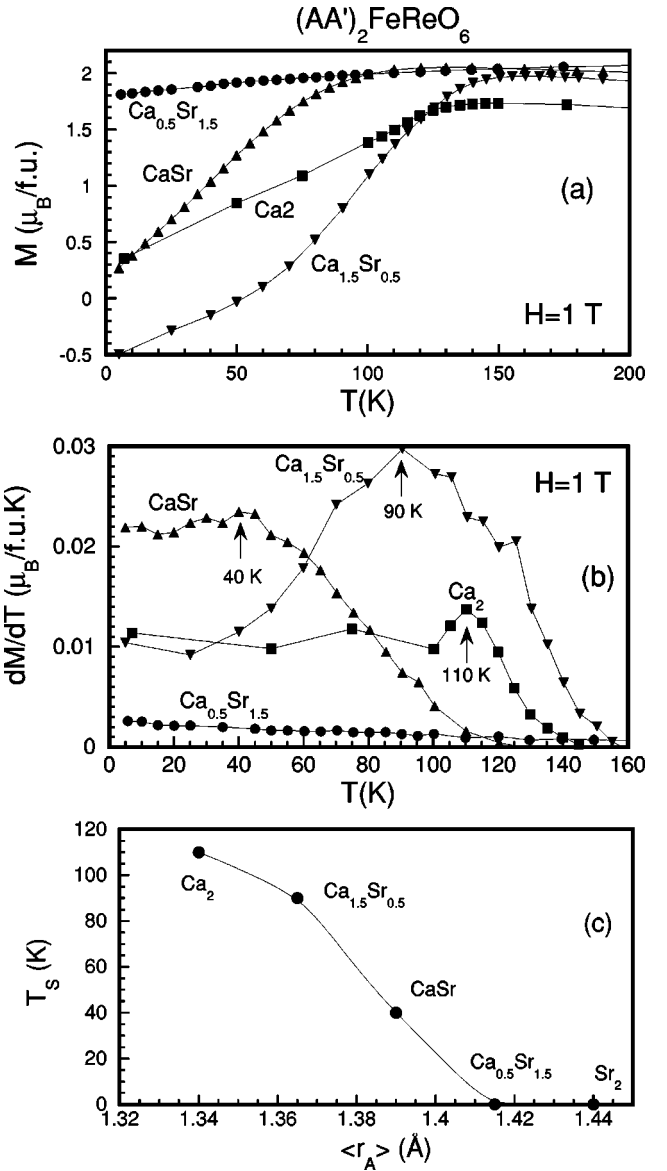


FIG. 6. (a) Magnetization versus temperature under 1 T for the compounds with small cation size. The samples were cooled without magnetic field down to 5 K. Afterwards, a  $-5$  T magnetic field was applied and, subsequently, the measuring field  $+1$  T was applied and the thermal dependence of the magnetization when heating was recorded. (b) The derivative of magnetization versus temperature for the compounds with small cation size is shown and the maximum is marked. (c) The transition temperature of the structural/magnetic transition obtained from the magnetic measurements is shown as a function of the cation size.

$M1$  phase, still present at 5 K.

In order to characterize precisely the transition temperature  $T_S$  from a magnetic point of view and the associated change in the coercive field, we have carried out the following experiment shown in Fig. 6. We cool down without applied magnetic field down to 5 K. Then, we saturate the magnetization by applying a *negative* magnetic field of 5 T. Afterwards, we apply a *positive* magnetic field of 1 T and we record the magnetization as a function of temperature by heating. In the case of compounds such as  $\text{Ca}_{0.5}\text{Sr}_{1.5}\text{FeReO}_6$ ,

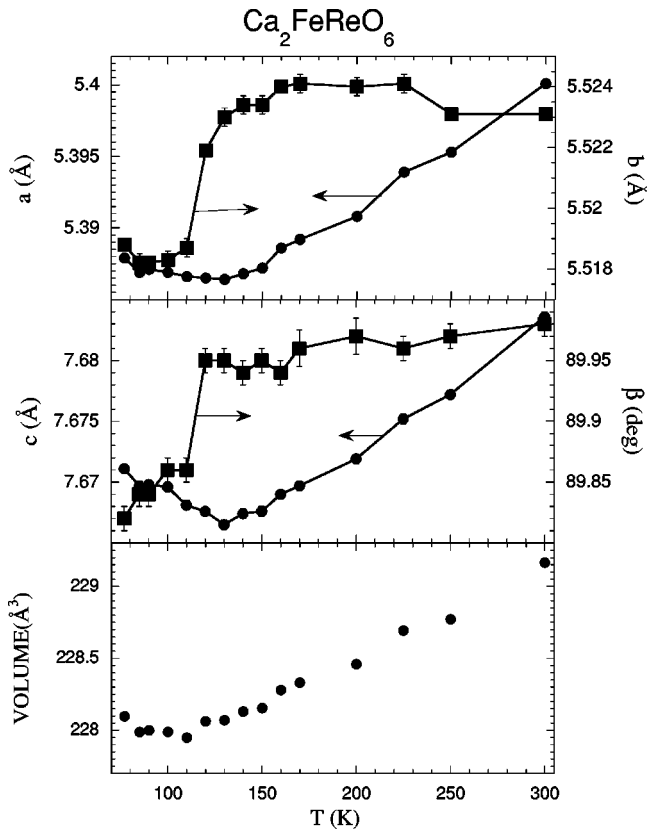


FIG. 7. Change in the cell parameters and volume as a function of temperature in  $\text{Ca}_2\text{FeReO}_6$ . Substantial variations are observed at  $T_S$ .

which does not undergo the structural/magnetic transition, a smooth thermal dependence of the magnetization is observed as expected from smooth variations of the “intrinsic” magnetization and the coercive field. However, in the compounds with smaller cation size ( $AA' = \text{CaSr}$ ,  $\text{Ca}_{1.5}\text{Sr}_{0.5}$ , and  $\text{Ca}_2$ ), strong variations of the recorded magnetization as a function of temperature are observed connected to the approaching  $T_S$ . The reason for the large variations in the recorded magnetization is not the variation in the “intrinsic” magnetization, which exists but is small, but the large change in coercivity occurring below  $T_S$ . Once  $T_S$  is overcome, a smooth variation in the recorded magnetization is again measured. By taking the derivative of these curves versus temperature, we can define  $T_S$  as the maximum of the derivative, which is shown in Fig. 6.

A striking difference between the series  $(AA')_2\text{FeReO}_6$  and  $(AA')_2\text{FeMoO}_6$  is the value of the coercive field. In the case of polycrystalline FeMo compounds, the coercive field is small (some tens of Oe),<sup>1,16</sup> as expected in ferromagnets with small anisotropy. In the case of polycrystalline FeRe compounds, the coercive field is very large. For the softer compound,  $\text{Ba}_2\text{FeReO}_6$ , it is  $\approx 1500$  Oe at 5 K and increases for the compounds with smaller cation size. This large coercivity brings about large remanent magnetization values as well. A substantially different microstructure in the FeRe compounds or the presence of plenty of defects cannot be invoked in order to explain the high coercivity. First, x-ray diffraction measurements do not detect any peak broadening

which could make suspect a substantial grain size change. Secondly, the large value of the attained saturation magnetization (very close to the maximum value) does not support the presence of many defects. As a consequence, the large coercivity must be attributed to a large intrinsic anisotropy of the FeRe compounds. A large intrinsic magnetic anisotropy can take place with an orbital anisotropic electron charge density (which couples to the lattice via crystal-field effects) and a spin-orbit interaction that couples the orbital and spin magnetic moments.<sup>24</sup> This mechanism requires a substantial spin-orbit coupling. In order to accomplish this mechanism, we suggest the existence of an unquenched orbital magnetic moment on the Re ion because it seems unrealistic that the Fe ions could bear a relevant orbital magnetic moment in these compounds. In that sense we can mention that the isostructural compound  $\text{Ca}_2\text{FeMoO}_6$  does not show magnetic properties analogous to those of  $\text{Ca}_2\text{FeReO}_6$ .<sup>16</sup> Moreover, Mössbauer experiments discard orbital effects of Fe in  $\text{Ca}_2\text{FeReO}_6$ .<sup>27</sup> Our results points to an increasing Re orbital moment as the cation size diminishes, which can be checked with x-ray magnetic circular dichroism measurements. The huge increase in the coercivity below  $T_S$  occurring in  $AA' = \text{CaSr}$ ,  $\text{Ca}_{1.5}\text{Sr}_{0.5}$ , and  $\text{Ca}_2$  can be connected with an enhanced orbital moment of the  $M2$  phase, which would make the magnetic anisotropy increase accordingly, or to an orbital ordering of the  $5d$  electrons in the Re ions as proposed by Oikawa *et al.*<sup>21</sup>

Low-temperature x-ray diffraction measurements have been carried out on  $\text{Ca}_2\text{FeReO}_6$  in order to further investigate the proposed magnetoelastic coupling. In Fig. 7 the thermal dependence of the individual lattice parameters, the  $\beta$  angle of the monoclinic unit cell, and the volume are shown. Before going into the structural details, we must recall that at  $T_S$  the easy magnetization axis changes from the  $ac$  plane to the  $b$  axis.<sup>20</sup> Our x-ray diffraction measurements indicate that large changes in the structural parameters occur at  $\approx 115$  K, which approximately coincides with  $T_S \approx 110$  K determined from magnetic measurements in this sample. We notice that at  $T_S$  the  $b$  axis shrinks whereas the  $a$  and  $c$  axis expand. Also, the  $\beta$  angle decreases reflecting a larger monoclinic distortion and the volume contracts. Again, a clear magnetoelastic effect is deduced. The fact of changing the easy magnetization axis to the  $b$  axis provokes a shrink of this axis and the expansion of the perpendicular axis. The magnetoelastic coupling occurring at  $T_S$  mimics the magnetoelastic coupling at  $T_C$ , which had also shown expansion of the axis perpendicular to the easy magnetization axis.

The main magnetotransport properties of the studied compounds are shown in Figs. 8–10. We do not observe any correlation between the absolute value of the room-temperature resistivity and the cation size. It typically varies between 0.05 and 1  $\Omega$  cm. However, a clear correlation between the cation size and the thermal dependence of resistivity is shown in Fig. 8. For the compounds with large cation size ( $AA' = \text{Ba}_2$  to  $\text{Sr}_2$ ) the resistance is slightly temperature dependent, at most a factor of 2 between low and room temperature. This is a typical behavior of polycrystalline metallic double perovskites like that of the samples belonging to  $(AA')_2\text{FeMoO}_6$  series.<sup>1</sup> However, with further decrease of

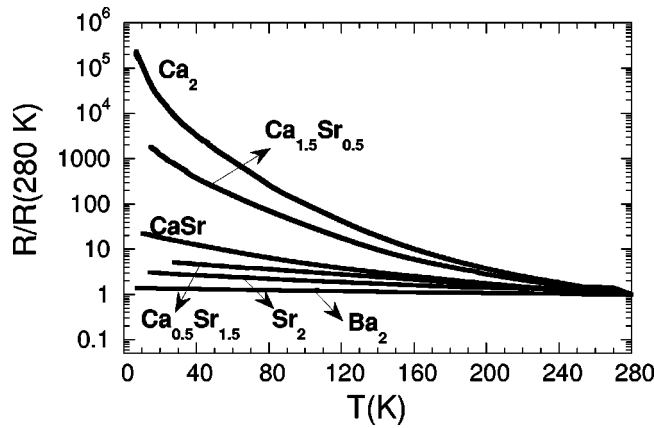


FIG. 8. Thermal dependence of the normalized resistivity for selected compounds (the resistivity has been normalized by the value at 250 K for the sake of clarity). Depending on the compound, the absolute value of resistivity at room temperature is typically between 0.05 and 1  $\Omega$  cm (without any clear dependence as a function of the cation size).

the cation size, a semiconducting tendency is developed. For example,  $\text{Ca}_2\text{FeReO}_6$  shows resistance at low temperatures a factor of  $10^5$  higher than at room temperature. Abrupt resistance changes at  $T_S$  are not observed (only a very small change of slope) and the semiconducting behavior remains in the whole temperature range. This means that both  $M1$  and  $M2$  phases share this semiconducting behavior even though  $M2$  seems to be slightly more insulating. Wu has proposed

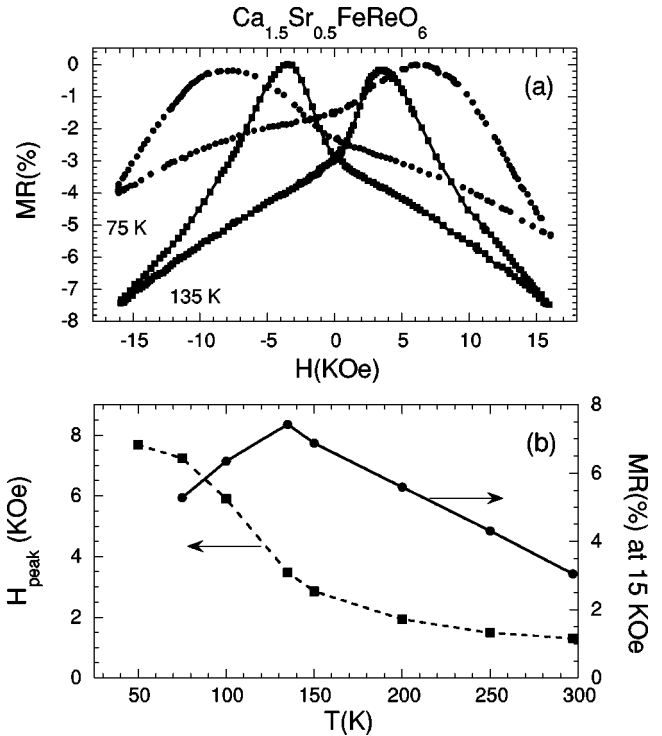


FIG. 10. (a) Magnetoresistance of  $\text{Ca}_{1.5}\text{Sr}_{0.5}\text{FeReO}_6$  at 75 and 135 K. (b) For the same compound, thermal dependence of the magnetoresistance and of the field ( $H_{\text{peak}}$ ) where the magnetoresistance peaks in the magnetoresistance isotherms.

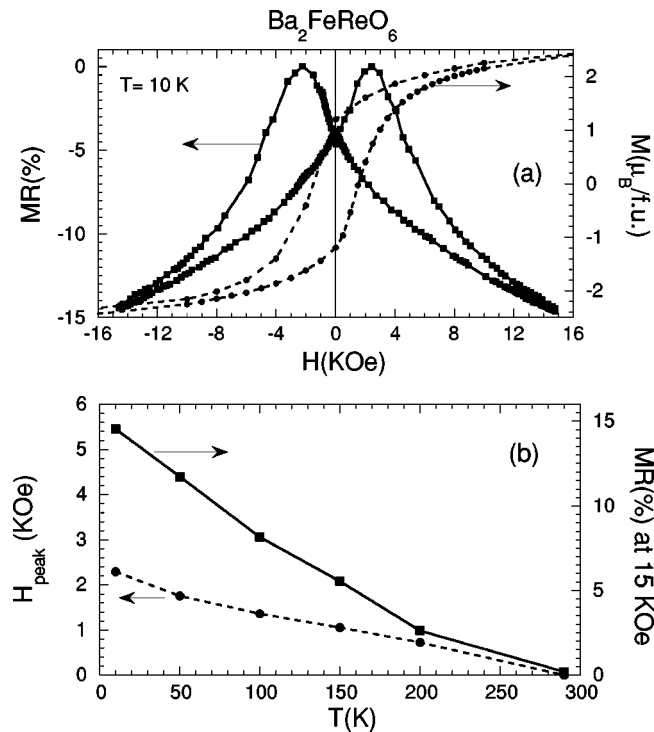


FIG. 9. (a) Magnetoresistance and magnetization of  $\text{Ba}_2\text{FeReO}_6$  at 10 K. (b) For the same compound, thermal dependence of the magnetoresistance and of the field ( $H_{\text{peak}}$ ) where the magnetoresistance peaks in the magnetoresistance isotherms.

that the loss of the metallic character in  $\text{Ca}_2\text{FeReO}_6$  can be related to the decrease in the  $(\text{Fe } t_{2g} - \text{Re } t_{2g}) pdd-\pi$  electronic transfer due to deviations of the Fe-O-Re angle off  $180^\circ$  in the monoclinic structure of this compound.<sup>17</sup>

Now we will focus on the impact of the magnetic properties on the magnetoresistance (MR) in this series of compounds. MR is defined as  $\text{MR}(\%) = 100 \times [\rho(H) - \rho(H_{\text{peak}})] / \rho(H)$ , where  $H_{\text{peak}}$  stands for the field at which the maximum  $\rho$  is reached. One of the most remarkable properties of polycrystalline double perovskites was the discovery of a large MR (Ref. 1) which is usually explained by the “intergrain magnetotunnelling” effect.<sup>29</sup> This mechanism is based on the fact that the grain boundary resistance can be modulated by an applied magnetic field if the conduction between grains proceeds via spin-dependent tunneling, which leads in some cases to a large MR. This occurs because at around zero field (more precisely, at the coercive field) the magnetization of neighboring grains is pointing randomly, which is a higher resistance state than having parallel magnetization between grains above the saturation field. A high spin polarization at the Fermi level is required to obtain large MR, as is the case in double perovskites.<sup>1</sup> In Fig. 9 we show the typical MR effects that we observed in the compounds with large cation size (as an example, we show the results of  $\text{Ba}_2\text{FeReO}_6$ ). Typical butterflylike shape is observed for the MR curves at fixed temperature.  $H_{\text{peak}}$  is found to be different to the coercive field ( $H_C$ ) measured in magnetization, but remains not too far. For the sake of comparison, the magnetization loop at the same temperature is

shown. However, we would like to remark that we always observe  $H_{\text{peak}}$  values higher than the corresponding  $H_C$ . As an example, in the case of  $\text{Ba}_2\text{FeReO}_6$  at 10 K we find  $H_{\text{peak}}=2.32$  KOe and  $H_C=1.51$  KOe. For intergrain MR, the relevant magnetization is that of the grain boundary. Our finding indicates that the grain boundary of these double perovskites is magnetically harder than the bulk. One possible reason for this effect is that the grain surface contains more density of defects than the bulk. Another possible reason is that the loss of the symmetry at the grain surface induces some electronic changes or magnetic surface anisotropy. As shown in Fig. 9,  $H_{\text{peak}}$  decreases smoothly with temperature (mimicking the behavior of  $H_C$ ) and vanishes at  $T_C$ . At 10 K the MR ratio at 15 KOe is 15% and decreases monotonically with temperature disappearing around  $T_C$ . Similar behavior of  $H_{\text{peak}}$  and MR is obtained for the rest of the compounds with large cation size. The MR ratios are quite high due to the high spin polarization at the Fermi level but the large coercive field of these compounds avoids the concentration of the MR effect at low fields. As a consequence, one would need higher magnetic fields in order to get the maximum feasible MR ratios. In contrast, in the  $(AA')_2\text{FeMoO}_6$  compounds the low values of the coercive field allows obtaining much larger MR ratios at low field.<sup>9,30,31</sup>

As concerns the samples with small cation size, the MR properties as a function of temperature are different due to the structural/magnetic transition at  $T_S$ . We illustrate this behavior with the results of  $\text{Ca}_{1.5}\text{Sr}_{0.5}\text{FeReO}_6$  ( $T_S \approx 90$  K), which are shown in Fig. 10. Our magnetic measurements have shown that the coercive field increases substantially at  $T_S$ . This has a strong impact on  $H_{\text{peak}}$  as can be seen in Fig. 9 and, as a consequence, on the MR loops (we show the loops at 75 and 135 K, i.e., above and below  $T_S$ ). Below  $T_S$  the maximum available field in our measurements (15 KOe) is not able to overcome the saturation field of the sample. This implies that, when doing the MR measurements up to 15 KOe, only minor loops are being carried out. This is the reason why the butterfly-shaped MR loop at 75 K is asymmetric. The huge increase in  $H_{\text{peak}}$  around  $T_S$  is also detrimental for the MR ratios. As shown in Fig. 10, when  $H_{\text{peak}}$  starts to increase in the vicinity of  $T_S$ , the MR at 15 KOe shows a maximum and then decreases. However, it is also true that the spin polarization of the low-temperature phase is unknown and could be different to that of the high-temperature phase. This could be another source for the diminution of the MR below  $T_S$ .

#### IV. DISCUSSION AND CONCLUSIONS

The structural, magnetic, and transport properties of the  $(AA')_2\text{FeReO}_6$  ( $AA' = \text{Ba}_2, \text{Ba}_{1.5}\text{Sr}_{0.5}, \text{BaSr}, \text{Ba}_{0.5}\text{Sr}_{1.5}, \text{Sr}_2, \text{Ca}_{0.5}\text{Sr}_{1.5}, \text{CaSr}, \text{Ca}_{1.5}\text{Sr}_{0.5}, \text{Ca}_2$ ) double perovskites have been studied in detail, which has allowed us to establish remarkable correlations between all these properties. In this series, the cation size plays a crucial role in the observed behavior. The compounds with large cation size ( $AA' = \text{Ba}_2, \text{Ba}_{1.5}\text{Sr}_{0.5}, \text{BaSr}, \text{Ba}_{0.5}\text{Sr}_{1.5}$ ) are cubic but with further cation size decrease the compounds become tetragonal ( $AA' = \text{Sr}_2$ ) and monoclinic ( $AA' = \text{Ca}_{0.5}\text{Sr}_{1.5}, \text{CaSr},$

$\text{Ca}_{1.5}\text{Sr}_{0.5}, \text{Ca}_2$ ). Anomalous behavior of the lattice parameters occur for the compounds with smaller cation size ( $AA' = \text{CaSr}, \text{Ca}_{1.5}\text{Sr}_{0.5}, \text{Ca}_2$ ), which is ascribed to a steric effect. This huge lattice effect combined with an unquenched Re orbital moment is probably responsible for the outstanding magnetic properties of these compounds. X-ray magnetic circular dichroism (XMCD) measurements would shed light on how the Re orbital moment evolves as a function of the cation size in this series.  $T_C$  increases with decreasing cation size in the cubic compounds as expected in the ferromagnetic double-exchange mechanism due to the increase of the electronic bare bandwidth owing to the diminution of the Fe/Re-O distance. However, an unexpected remarkable increase of  $T_C$  occurs in the tetragonal/monoclinic compounds which cannot be explained by the same mechanism because the Fe-O-Re angle deviates from  $180^\circ$ . This will disturb the  $(\text{Fe}t_{2g} - \text{Re}t_{2g})pdd-\pi$  coupling. Instead, this departure from  $180^\circ$  can allow the  $(\text{Fe}e_g - \text{Re}e_g)pdd-\sigma$  coupling, which has been invoked by Wu in  $\text{Ca}_2\text{FeReO}_6$  as a source of increasing the ferromagnetic coupling.<sup>17</sup>

Magnetization measurements at 5 K indicate that the saturation magnetization is close to  $3\mu_B/\text{f.u.}$  for the compounds with large cation size ( $AA' = \text{Ba}_2, \text{Ba}_{1.5}\text{Sr}_{0.5}, \text{BaSr}, \text{Ba}_{0.5}\text{Sr}_{1.5}, \text{Sr}_2, \text{Ca}_{0.5}\text{Sr}_{1.5}$ ), which is compatible with the ferrimagnetic coupling of the Fe and Re sublattices and both electronic configurations  $\text{Fe}^{+3}-\text{Re}^{+5}$  and  $\text{Fe}^{+2}-\text{Re}^{+6}$ . NMR and Mössbauer experiments are also consistent with these electronic configurations. The coercive field is in all cases large (much larger than in  $AA'\text{FeMoO}_6$  double perovskites), in the KOe range. This is thought to arise from a large magnetic anisotropy due to an unquenched Re orbital moment together with crystal-field interaction and spin-orbit coupling. In the compounds with small cation size ( $AA' = \text{CaSr}, \text{Ca}_{1.5}\text{Sr}_{0.5},$  and  $\text{Ca}_2$ ) the magnetic behavior is more complicate, especially due to a magnetic/structural transition occurring at  $T_S$  below 150 K. The following picture could explain the unconventional behavior of these small cation size compounds. In these compounds two different phases of similar energy,  $M1$  and  $M2$ , are competing to be the ground state.  $M1$  is predominant above  $T_S$  and  $M2$  below  $T_S$  but both phases can coexist in a wide temperature range as has been demonstrated in  $\text{Ca}_2\text{FeReO}_6$  by means of neutron diffraction.<sup>12,20</sup> Both phases have different magnetic and electronic properties. Concerning the magnetic properties,  $M1$  is a collinear ferrimagnet (Re magnetic moment antiparallel to the Fe magnetic moment) with saturation magnetization of  $3\mu_B/\text{f.u.}$  and the easy magnetization axis lies in the  $ac$  plane.  $M2$  shows a ferrimagnetic ordering with an antiferromagnetic canting and the magnetization under 5 T is lower than  $3\mu_B/\text{f.u.}$  The easy magnetization axis of  $M2$  is parallel to the  $b$  axis. By inspection of the individual behavior of the lattice parameters as a function of the cation size and temperature, we propose a strong magnetoelastic coupling in both  $M1$  and  $M2$  phases, which is a consequence of an unquenched Re orbital moment.  $M1$  shows a large coercive field (as in the compounds with large cation size) which is attributed to a large magnetic anisotropy produced by the Re orbital moment. In  $M2$  the coercive field is huge (up to



one order of magnitude larger than in  $M1$ ) which can imply that the Re orbital moment is larger in  $M2$  than in  $M1$ . If this is true, one would expect to detect electronic changes at  $T_S$ , when  $M2$  becomes predominant in the sample. This assumption is supported by Mössbauer experiments that indicate at  $T_S$  a change of the electronic state of Fe from  $\text{Fe}^{+2.5}$  towards  $\text{Fe}^{+3}$  in  $\text{Ca}_2\text{FeReO}_6$  (Ref. 27) and by optical conductivity measurements that detect the opening of a gap at the Fermi level at  $T_S$  for this compound. Again, XMCD experiments could further investigate the change in the orbital moment at  $T_S$ . Low-temperature x-ray diffraction measurements in  $\text{Ca}_2\text{FeReO}_6$  allow the detection of strong anomalies in the lattice parameters associated to the  $M1 \rightarrow M2$  transition occurring at  $T_S$ . Granado *et al.* have found that the magnetic field influences the relative amount of the  $M1$  and  $M2$  phases.<sup>20</sup> As we have found different magnetoelastic coupling in the  $M1$  and  $M2$  phases, one can anticipate large magnetostrictive effects by application of magnetic field. In fact, preliminary measurements in our  $\text{Ca}_2\text{FeReO}_6$  sample indicate large magnetostriction at 12 T, in the range of 0.1%.<sup>32</sup>

Transport measurements show a trend towards insulating behavior as the cation size diminishes. Magnetoresistance experiments in our polycrystalline samples show large intergrain MR persisting up to  $T_C$ . The effect is burdened by the large coercive fields. In the MR isotherms, the resistance has a maximum at a field  $H_{\text{peak}}$ , which is always larger than the  $H_C$  observed in magnetization measurements. In the compounds with small cation size the MR decreases below  $T_S$  due to the huge coercivity of the low-temperature phase.

In conclusion, these results clarify the role played by the cation size in the structural, magnetic and magnetotransport properties of  $AA'\text{FeReO}_6$  double perovskites. An additional ferromagnetic mechanism to the usual  $(\text{Fe}t_{2g} - \text{Re}t_{2g})pdd-\pi$  coupling must be invoked in order to explain the high  $T_C$  observed in the compounds with small cation size. An unquenched Re orbital moment seems to be responsible for the large coercive fields found in these compounds. The structural and magnetic behavior of the compounds with small cation size ( $AA' = \text{CaSr}$ ,  $\text{Ca}_{1.5}\text{Sr}_{0.5}$ , and  $\text{Ca}_2$ ) suggests a strong magnetoelastic coupling. Two different phases ( $M1$  and  $M2$ ) with different magnetic properties compete in the latter compounds and a simultaneous structural/magnetic transition between these phases occurs at  $T_S$ . Large magnetostrictive effects with applied magnetic field are anticipated due to the large magnetoelastic coupling and the competition between the  $M1$  and  $M2$  phases. Once an unquenched Re orbital moment has been established, one open question is whether some type of orbital ordering exists in these compounds. At this stage, one cannot draw definitive conclusions and further experiments with specific techniques (x-ray resonant scattering) should be tried.

#### ACKNOWLEDGMENTS

Financial support by the European Commission through the European Projects AMORE and SCOOTMO and by the Spanish Ministry of Science and Technology (Grant Nos. MAT2002-04657 and MAT2002-01221, including FEDER funding) is acknowledged.

- 
- <sup>1</sup>K.-I. Kobayashi, T. Kimura, H. Sawada, K. Terakura, and Y. Tokura, *Nature (London)* **395**, 677 (1998).
- <sup>2</sup>K.-I. Kobayashi, T. Kimura, Y. Tomioka, H. Sawada, K. Terakura, and Y. Tokura, *Phys. Rev. B* **59**, 11 159 (1999).
- <sup>3</sup>R. P. Borges, R. M. Thomas, C. Cullinan, J. M. D. Coey, R. Suryanarayanan, L. Ben-Dor, L. Pinsard-Gaudart, and A. Revcholschi, *J. Phys.: Condens. Matter* **11**, L445 (1999).
- <sup>4</sup>T. H. Kim, M. Uehara, S.-W. Cheong, and S. Lee, *Appl. Phys. Lett.* **74**, 1737 (1999).
- <sup>5</sup>J. Navarro, C. Frontera, Ll. Balcells, B. Martínez, and J. Fontcuberta, *Phys. Rev. B* **64**, 092411 (2001).
- <sup>6</sup>J. B. Philipp, D. Reisinger, M. Schonecke, A. Marx, A. Erb, L. Alff, R. Gross, and J. Klein, *Appl. Phys. Lett.* **79**, 3654 (2001).
- <sup>7</sup>J. Gopalakrishnan, A. Chattopadhyay, S. B. Ogale, T. Venkatesan, R. L. Greene, A. J. Millis, K. Ramesha, B. Hannoyer, and G. Marest, *Phys. Rev. B* **62**, 9538 (2000).
- <sup>8</sup>W. Prellier, V. Smolyaninova, A. Biswas, C. Galley, R. L. Greene, K. Ramesha, and J. Gopalakrishnan, *J. Phys.: Condens. Matter* **12**, 9538 (2000).
- <sup>9</sup>Bog-Gi Kim, Yew-San Hor, and S.-W. Cheong, *Appl. Phys. Lett.* **79**, 388 (2001).
- <sup>10</sup>H. Kato, T. Okuda, Y. Okimoto, Y. Tomioka, Y. Takenoya, Y. Ohkubo, M. Kawasaki, and Y. Tokura, *Appl. Phys. Lett.* **81**, 328 (2002).
- <sup>11</sup>T. Alamelu, U. V. Varadaraju, M. Venkatesan, A. P. Douvalis, and J. M. D. Coey, *J. Appl. Phys.* **91**, 8909 (2002).
- <sup>12</sup>W. Westerburg, O. Lang, C. Ritter, C. Felser, W. Tremel, and G. Jakob, *Solid State Commun.* **122**, 201 (2002).
- <sup>13</sup>H. Kato, T. Okuda, Y. Okimoto, Y. Tomioka, K. Oikawa, T. Kamiyama, and Y. Tokura, *Phys. Rev. B* **65**, 144404 (2002).
- <sup>14</sup>M. Bibes, K. Bouzehouane, A. Barthelemy, M. Besse, S. Fusil, M. Bowen, P. Seneor, J. P. Contour, and A. Fert, *Appl. Phys. Lett.* **83**, 2629 (2003).
- <sup>15</sup>J. Fontcuberta *et al.*, *J. Magn. Magn. Mater.* **242**, 98 (2002).
- <sup>16</sup>C. Ritter, M. R. Ibarra, L. Morellon, J. Blasco, J. García, and J. M. De Teresa, *J. Phys.: Condens. Matter* **12**, 8295 (2000).
- <sup>17</sup>H. Wu, *Phys. Rev. B* **64**, 125126 (2001).
- <sup>18</sup>D. Serrate, J. M. De Teresa, J. Blasco, M. R. Ibarra, L. Morellon, and C. Ritter (unpublished).
- <sup>19</sup>Guerman Popov, Martha Greenblatt, and Mark Croft, *Phys. Rev. B* **67**, 024406 (2003).
- <sup>20</sup>E. Granado, Q. Huang, J. W. Lynn, J. Gopalakrishnan, R. L. Greene, and K. Ramesha, *Phys. Rev. B* **66**, 064409 (2002).
- <sup>21</sup>K. Oikawa, T. Kamiyama, H. Kato, and Y. Tokura, *J. Phys. Soc. Jpn.* **72**, 1411 (2003).
- <sup>22</sup>P. M. Woodward, *Acta Crystallogr., Sect. B: Struct. Sci.* **53**, 32 (1997).
- <sup>23</sup>R. D. Shannon, *Acta Crystallogr., Sect. A: Cryst. Phys., Diff., Theor. Gen. Crystallogr.* **32**, 751 (1976).
- <sup>24</sup>A. del Moral, P. A. Algarabel, J. I. Arnaudas, L. Benito, M. Ciria,

- C. de la Fuente, B. García-Landa, M. R. Ibarra, C. Marquina, L. Morellon, and J. M. De Teresa, *J. Magn. Magn. Mater.* **242–245**, 788 (2002).
- <sup>25</sup>A. W. Sleight and J. F. Weiher, *J. Phys. Chem. Solids* **33**, 679 (1972).
- <sup>26</sup>F. Sriti, N. Nguyen, C. Martin, A. Ducouret, and B. Raveau, *J. Magn. Magn. Mater.* **250**, 123 (2002).
- <sup>27</sup>S. Nakamura, M. Tanaka, H. Kato, and Y. Tokura, *J. Phys. Soc. Jpn.* **72**, 424 (2003).
- <sup>28</sup>Cz. Kapusta *et al.* (unpublished).
- <sup>29</sup>H. Y. Hwang, S.-W. Cheong, N. P. Ong, and B. Batlogg, *Phys. Rev. Lett.* **77**, 2041 (1996).
- <sup>30</sup>J. P. Zhou, R. Dass, H. Q. Yin, J.-S. Zhou, L. Rabenberg, and J. B. Goodenough, *J. Appl. Phys.* **87**, 5037 (2000).
- <sup>31</sup>D. Serrate, J. M. De Teresa, J. Blasco, M. R. Ibarra, L. Morellon, and C. Ritter, *Appl. Phys. Lett.* **80**, 4573 (2002).
- <sup>32</sup>D. Serrate *et al.* (unpublished).